

Electron-spin-resonance study of Sn⁺(5p1) centers of the laser-active-type structure in KCl:Sn²⁺ and analysis of the hyperfine structure

Citation for published version (APA):

Schoemaker, D., Heynderickx, I. E. J., & Goovaerts, E. (1985). Electron-spin-resonance study of Sn⁺(5p1) centers of the laser-active-type structure in KCl:Sn²⁺ and analysis of the hyperfine structure. *Physical Review B: Condensed Matter*, 31(9), 5687-5693. <https://doi.org/10.1103/PhysRevB.31.5687>

DOI:

[10.1103/PhysRevB.31.5687](https://doi.org/10.1103/PhysRevB.31.5687)

Document status and date:

Published: 01/01/1985

Document Version:

Publisher's PDF, also known as Version of Record (includes final page, issue and volume numbers)

Please check the document version of this publication:

- A submitted manuscript is the version of the article upon submission and before peer-review. There can be important differences between the submitted version and the official published version of record. People interested in the research are advised to contact the author for the final version of the publication, or visit the DOI to the publisher's website.
- The final author version and the galley proof are versions of the publication after peer review.
- The final published version features the final layout of the paper including the volume, issue and page numbers.

[Link to publication](#)

General rights

Copyright and moral rights for the publications made accessible in the public portal are retained by the authors and/or other copyright owners and it is a condition of accessing publications that users recognise and abide by the legal requirements associated with these rights.

- Users may download and print one copy of any publication from the public portal for the purpose of private study or research.
- You may not further distribute the material or use it for any profit-making activity or commercial gain
- You may freely distribute the URL identifying the publication in the public portal.

If the publication is distributed under the terms of Article 25fa of the Dutch Copyright Act, indicated by the "Taverne" license above, please follow below link for the End User Agreement:

www.tue.nl/taverne

Take down policy

If you believe that this document breaches copyright please contact us at:

openaccess@tue.nl

providing details and we will investigate your claim.

Electron-spin-resonance study of $\text{Sn}^+(5p^1)$ centers of the laser-active-type structure in $\text{KCl}:\text{Sn}^{2+}$ and analysis of the hyperfine structure

D. Schoemaker, I. Heynderickx, and E. Goovaerts

Physics Department, University of Antwerp (U.I.A.), B-2610 Wilrijk-Antwerp, Belgium

(Received 30 November 1984)

It is shown through an analysis of the electron-spin-resonance spectra that the $\text{Sn}^{2+}(5s^2)$ impurities in KCl can also give rise, after x irradiation above 220 K, to the so-called $\text{Sn}^+(1)$ centers of the laser-active-type structure. The essential core of this center is a substitutional $\text{Sn}^+(5p^1)$ ion strongly perturbed by an adjoining anion vacancy along the $\langle 001 \rangle$ direction. The observed orthorhombic symmetry, with the three crystallographic axes as the main axes, is induced by either one or two weakly perturbing cation vacancies in the neighborhood. Their exact positions are hard to establish and several possible, subtly differing, defect models are proposed. An analysis of the hyperfine interaction of all the np^1 ($n=4,5,6$) centers in KCl is presented, and it is established that these atoms and ions possess large negative unpaired electron-spin densities at their nuclei when they are free or in crystal fields possessing inversion symmetry. The strong odd field component induced by the anion vacancy invariably adds, through s mixing, a substantial positive contribution to this spin density.

I. INTRODUCTION

The electron-spin-resonance (ESR) studies of $\text{Sn}^+(5p^1)$ (Ref. 1) and $\text{Sn}^-(5p^3)$ (Refs. 2 and 3) centers in x-irradiated $\text{Sn}^{2+}(5s^2)$ -doped alkali halides have contributed a great deal of information about the mobility of cation and anion vacancies. The realization¹⁻⁴ that, similar to cation vacancies, the anion vacancies become quite mobile above 220 K in KCl was very important in establishing the model of the so-called $\text{Tl}^0(1)$ center in $\text{Tl}^+(6s^2)$ -doped alkali halides.⁵⁻⁷ In this center, a $\text{Tl}^0(6p^1)$ atom (produced through the trapping of electron by a Tl^+ ion on a cation site) is perturbed by an adjoining anion vacancy along a $\langle 100 \rangle$ direction. This vacancy exerts a strong perturbation of the Tl^0 , e.g., influencing in a very specific way its hyperfine (hf) interaction.⁵ Furthermore, the perturbing anion vacancy, inducing a strong odd crystal field, is also responsible for making optical transitions weakly allowed between the spin-orbit- and crystal-field-split L - S ground manifold of the $\text{Tl}^0(6p^1)$ atom.^{8,9} Pumping this transition at $1.05 \mu\text{m}$ with a Nd:Yag (YAG denotes yttrium-aluminum-garnet) laser results in strong luminescence at $1.5 \mu\text{m}$ from which high-intensity near-infrared mode-locked lasers have been produced,^{10,11} recently yielding femtosecond pulses.¹² As a result, the $\text{Tl}^0(1)$ center is also called the laser-active $\text{Tl}^0(1)$ center, and other heavy-metal-ion centers possessing a similar defect structure are called "centers possessing the laser-active-type structure." Centers having such a structure need not necessarily be laser-active, as is clearly demonstrated by the $\text{Ga}^0(1)$ and $\text{In}^0(1)$ centers^{13,14} in KCl, which do not luminesce and lase.¹⁵ It has been shown that within the framework of the Dexter-Klick-Russell rule, the smaller spin-orbit interaction of $\text{Ga}^0(4p^1)$ and $\text{In}^0(5p^1)$ compared to $\text{Tl}^0(6p^1)$ is responsible for this.¹⁶

It is clearly interesting to expand these studies to the ns^2 ($n=4,5,6$) divalent Ge^{2+} , Sn^{2+} , and Pb^{2+} impurities

which run parallel to the monovalent Ga^+ , In^+ , and Tl^+ series. The Ge^{2+} ion is difficult to incorporate in the alkali halides and little is known about it. However, it is well established that Sn^{2+} and Pb^{2+} are excellent electron (and hole^{17,18} and interstitial¹⁹) traps yielding $\text{Sn}^+(5p^1)$ (Ref. 1) and $\text{Pb}^+(6p^1)$ (Ref. 20) defects in the alkali halides. It should be possible to produce $\text{Sn}^+(1)$ and $\text{Pb}^+(1)$ centers of the laser-active structure, and this is confirmed for $\text{Sn}^+(1)$ in this paper. In Sec. III the ESR spectra of $\text{Sn}^+(1)$ are identified and analyzed.

A complicating feature of the divalent impurity-doped crystals is the presence of charge-compensating cation vacancies. This gives rise, in principle, to a great variety of cation-vacancy-perturbed defects, and this is discussed in Sec. IV. In Sec. V a few thermal, optical, and production properties of $\text{Sn}^+(1)$ are presented. Finally, in Sec. VI a detailed analysis is presented of the hyperfine interaction of all the np^1 ($n=4,5,6$) atom and ion centers studied so far in KCl, and some interesting regularities in the hf behavior will be demonstrated.

II. EXPERIMENTAL DETAILS

The $\text{KCl}:\text{Sn}^{2+}$ crystals were the same as the ones used in the Sn^+ and Sn^- investigations.^{1,2} The KCl crystals were doped in the melt with about 1 wt. % of SnCl_2 . The tin hyperfine structure was studied in a KCl crystal doped with 90% isotope-enriched ^{119}Sn , whose nuclear spin is $\frac{1}{2}$. The defects were created by x-irradiating the samples for about 15 min at temperatures between 200 and 320 K using a tube with a tungsten target operating at 50 kV and 50 mA. Before every irradiation the samples were routinely heated to about 600°C for several minutes, after which they were rapidly cooled to room temperature or below. Experimental details on the electron-spin-resonance measurements can be found in Ref. 2.

III. ANALYSIS OF THE $\text{Sn}^+(1)$ ESR SPECTRA

The center which we will call the $\text{Sn}^+(1)$ center is most strongly produced at about 250 K by a 10-min x irradiation of a $\text{KCl}:\text{Sn}^{2+}$ crystal (see Sec. V). Such an irradiation also creates the SnCl_2^- (tetrag) centers,¹ the Sn^- centers,² and the Sn^{3+} centers,¹⁸ which are all observable in ESR. Figure 1 shows the $\text{Sn}^+(1)$ ESR spectrum at 77 K with the static magnetic field $\mathbf{H} \parallel \langle 100 \rangle$. It consists of a strongly anisotropic line which exhibits a four-line superhyperfine (shf) structure. Ignoring this structure for a moment, the single line originates from the even- A Sn isotopes possessing no nuclear spin and which account for 83.8% of the total natural tin abundance. The two odd isotopes ^{117}Sn (7.51%) and ^{119}Sn (8.45%) both possess nuclear spin $I_1 = \frac{1}{2}$ with very nearly the same nuclear moments, i.e., $\mu_N(^{117}\text{Sn}) = -0.9951$ and $\mu_N(^{119}\text{Sn}) = -1.0411$ nuclear magnetons. The weak corresponding hf doublets can be discerned in Fig. 1(a), but more convincing evidence is presented in Fig. 1(b), where the

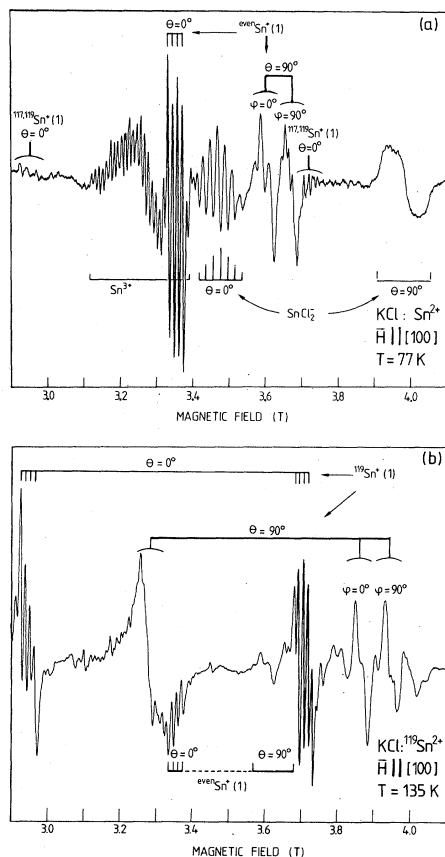


FIG. 1. ESR spectra of the $\text{Sn}^+(1)$ center in KCl for $\mathbf{H} \parallel \langle 100 \rangle$. Spectrum (a), taken at 77 K, shows the even $\text{Sn}^+(1)$ center in KCl doped with nonenriched Sn^{2+} ; the resolved spectra of Sn^{3+} and Sn^+ (tetrag) $\equiv \text{SnCl}_2^-$ are also indicated. Spectrum (b) exhibits the dominant hyperfine doublet of $^{119}\text{Sn}^+(1)$ in KCl doped with 90% enriched $^{119}\text{Sn}^{2+}$; this spectrum was recorded at 135 K, where $^{119}\text{Sn}^+(1)$, though weaker and somewhat more distorted than at 77 K, appears relatively stronger than Sn^{3+} and Sn^+ (tetrag), whose lines have broadened significantly.

$^{119}\text{Sn}^+(1)$ ESR spectrum is shown at 135 K in a $\text{KCl}:\text{Sn}^{2+}$ crystal containing 90% of the enriched ^{119}Sn isotope. The hf doublet now dominates the spectrum and each component again exhibits the four-line shf structure.

An angular variation and a quantitative study show that the $\text{Sn}^+(1)$ ESR spectrum possesses orthorhombic symmetry with the principal axes (x, y, z) coinciding, or very nearly coinciding, with the three $\langle 100 \rangle$ crystallographic axes. The $\text{Sn}^+(1)$ spectra in Figs. 1(a) and (b) are designated by the polar angles (θ, φ) that \mathbf{H} makes with the principal axes of the center. Only when \mathbf{H} is accurately parallel to the $\langle 100 \rangle$ direction is the four-line shf structure clearly resolved in the $\theta=0^\circ$ line. Turning \mathbf{H} away from the $\langle 100 \rangle$ direction by not more than 2° completely garbles the shf structure and it is not recovered at larger angles. This could indicate that the z axis of $\text{Sn}^+(1)$ is tipped by a very small angle away from a $\langle 100 \rangle$ direction in a $\{100\}$ plane. An attempt to estimate this angle yields an upper limit of 3° . Another explanation (see Sec. IV) could be that there is more than one $\text{Sn}^+(1)$ -type center that, because their structures are only subtly different, yield exactly the same $\theta=0^\circ$ spectra, but not, e.g., $\theta=90^\circ$ spectra. In fact, the $\theta=90^\circ, \varphi=0^\circ$ line in Fig. 1(a) exhibits a doublet structure which can be interpreted in two ways: either it originates from an unresolved four-line shf structure of similar origin as the $\theta=0^\circ$ line, or it represents two different $\theta=90^\circ, \varphi=0^\circ$ lines of two slightly different $\text{Sn}^+(1)$ centers. The latter interpretation yields 1.841 and 1.800 as the two g_x values. A similar analysis can be made for the $\theta=90^\circ, \varphi=90^\circ$ lines in Fig. 1(a) and for the tin hf lines in Fig. 1(b). If this interpretation were correct, then the $a_\perp(^{35}\text{Cl})$ value in Table I must be replaced by $a_\perp(^{35}\text{Cl}) \approx 0$ mT.

Unfortunately we have not been able to prove or disprove, through a pulse-anneal experiment, the existence of two slightly different $\text{Sn}^+(1)$ ESR spectra, because, e.g., the $\theta=90^\circ, \varphi=0^\circ$ "doublet" seems to decay as a whole in the (250–300)-K region (Sec. V). Even if there would be two slightly different $\text{Sn}^+(1)$ -type centers, the great similarity in their structure (see Sec. IV) makes it plausible that they possess decay temperatures which are very close together.

The Sn^+ (tetrag) center possesses a seven-line shf structure [see Fig. 1(a)] and this was shown¹ to originate from interaction with two equivalent chlorine nuclei. Both ^{35}Cl (75% abundant) and ^{37}Cl (25% abundant) possess nuclear spin $I_2 = \frac{3}{2}$ with very comparable nuclear moments. Similarly, the four-line shf structure of $\text{Sn}^+(1)$ undoubtedly arises from interaction with a single Cl nucleus.

The $\text{Sn}^+(1)$ ESR spectra were fitted to the spin Hamiltonian (usual notation):

$$\mathcal{H}/g_0\mu_B = \frac{1}{g_0} \mathbf{H} \cdot \vec{g} \cdot \mathbf{S} + \mathbf{S} \cdot \vec{A} \cdot \mathbf{I}_1 + \mathbf{S} \cdot \vec{a} \cdot \mathbf{I}_2, \quad (1)$$

and the results are presented in Table I. The ^{35}Cl and ^{37}Cl isotope effects are not resolved in the four-line shf structure, but ^{35}Cl is the dominant species. For comparison, in Table I we include the Sn^+ (tetrag) data.¹

Table I leaves no doubt about the fact that the basic entity in the $\text{Sn}^+(1)$ is indeed a $\text{Sn}^+(5p^1)$ species, as we have accepted all along. The $\text{Sn}^+(1)$ g factors are qualitatively

TABLE I. Spin-Hamiltonian parameters of $\text{Sn}^+(1)$ in $\text{KCl}:\text{Sn}^{2+}$ at 77 K. For comparison, the $\text{Sn}^+(\text{tetrag})$ parameters (Ref. 1) are included. The hyperfine parameters and the linewidths ΔH are given in mT.

Center	g_x [100]	g_y [010]	g_z [001]	$A_x(^{119}\text{Sn})$ [100]	$A_y(^{119}\text{Sn})$ [010]	$A_z(^{119}\text{Sn})$ [001]	$a_1(^{35}\text{Cl})$	$a_2(^{35}\text{Cl})$ [001]	ΔH
$\text{Sn}^+(1)^a$	1.819 ± 0.001	1.788 ± 0.001	1.9591 ± 0.0005	+52.9 ± 0.1	+53.8 ± 0.1	-73.0 ± 0.1	1.0 ^b ± 0.1	1.29 ± 0.2	0.60 ^c ± 0.05
$\text{Sn}^+(\text{tetrag})^d$	1.6494 ± 0.0002		1.8952 ± 0.0002	+93.3 ± 0.2		-82.8 ± 0.6	1.43 ± 0.05	1.99 ± 0.01	0.30 ^c ± 0.05

^aThe $\text{Sn}^+(1)$ center may be viewed as a SnCl molecule exhibiting hf interaction with a single Cl nucleus.

^bIn case there are two $\text{Sn}^+(1)$ centers, it is possible that $a_1(\text{Cl}) \approx 0$ mT (see Sec. III).

^cFor the resolved $\theta=0^\circ$ spectrum.

^dThe $\text{Sn}^+(\text{tetrag})$ center may be viewed as a symmetric linear SnCl_2^- molecule exhibiting hf interaction with two equivalent Cl nuclei.

and quantitatively quite similar to those of $\text{Sn}^+(\text{tetrag})$, which, in a simple crystal-field picture, are described by¹³

$$\Delta g_{\parallel} = g_0 - g_{\parallel} = \lambda^2/E^2, \quad \Delta g_{\perp} = g_0 - g_{\perp} = 2\lambda/E + 2\lambda^2/E^2, \quad (2)$$

where $\lambda \approx 2.800 \text{ cm}^{-1}$ is the spin-orbit-coupling constant¹ of Sn^+ , and E is the energy splitting between the p_z ground state (or corresponding molecular orbital) and the excited p_x, p_y excited orbitals (or molecular orbitals). The quantitative fit of formulas (2) to the experimental data of Table I leaves something to be desired, but this can be attributed to the simplicity of the model.

Both the ^{119}Sn and Cl hf interactions are somewhat smaller in $\text{Sn}^+(1)$ compared to $\text{Sn}^+(\text{tetrag})$. Little more can be said at this point about the Cl shf interaction. The ^{119}Sn hf will be analyzed in Sec. VI and an important conclusion will be drawn there: In $\text{Sn}^+(1)$ the Sn^+ ion is positioned in a strong odd axial crystal field along a $\langle 100 \rangle$ direction, whereas for $\text{Sn}^+(\text{tetrag})$ the crystal field is strictly even.

IV. MODELS FOR THE $\text{Sn}^+(1)$ CENTERS

A. The essential core: The laser-active-type structure

The ESR analysis clearly shows that the $\text{Sn}^+(1)$ center consists of a single Sn^+ ion interacting preferentially with a single Cl nucleus and that it possesses orthorhombic symmetry with the $\langle 100 \rangle$ crystallographic axes as main axes. A very small tipping ($< 3^\circ$) of the z axis may or may not exist. An important observation (Sec. V) is that $\text{Sn}^+(1)$ can only be produced by an x irradiation above 220 K, i.e., the temperature region in which anion vacancies become increasingly mobile. It shares this property with the $\text{Tl}^0(1)$, $\text{In}^0(1)$, $\text{Ga}^0(1)$, Sn^- , and Pb^- centers,^{2,3,5,6,13,14} and this convincingly indicates that an anion vacancy is involved in the $\text{Sn}^+(1)$ structure. Finally, the analysis of the ^{119}Sn hf structure in Sec. VI shows that the Sn^+ in $\text{Sn}^+(1)$ experiences a strong odd component of an essentially axial crystal field along a $\langle 100 \rangle$ direction.

Based on the above facts, in Fig. 2 we present what we believe is the essential core of the $\text{Sn}^+(1)$ center and we

will designate it as " $\text{Sn}^+(1)$." This model is identical to the laser-active $\text{Tl}^0(1)$ center with Sn^+ substituting for Tl^0 , i.e., the " $\text{Sn}^+(1)$ " structure is a "laser-active-type structure" as defined in the Introduction. The Sn^+ is flanked on one side by an anion vacancy and on the other by a substitutional Cl^- ion. The nucleus of the latter is responsible for the four-line shf structure and its presence points to a—probably weak—molecular bond between Sn^+ and Cl^- . This is indicated in Fig. 2 by a somewhat arbitrary contour. The anion vacancy also induces the strong, odd crystal-field component along the [100] direction whose presence is derived from an analysis of the $^{119}\text{Sn}^+$ hyperfine structure (Sec. VI).

The " $\text{Sn}^+(1)$ " core model possesses tetragonal symmetry around the [001] axis, and, as such, it cannot represent the complete model for the orthorhombic $\text{Sn}^+(1)$ center.

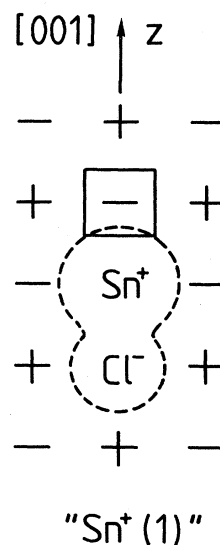


FIG. 2. Essential structural core of the $\text{Sn}^+(1)$ center(s) presented in a (100) plane showing a Sn^+ center strongly perturbed by an anion vacancy. An actual center like this core, called " $\text{Sn}^+(1)$ " has not been observed. In the observed orthorhombic $\text{Sn}^+(1)$ center a perturbing entity must be present nearby in the (100) plane. Possible actual models are presented in Fig. 3.

It is clear that the “ $\text{Sn}^+(1)$ ” core must be weakly perturbed by something else in the vicinity. The cation vacancies present in the crystal as the original charge compensators for the Sn^{2+} impurities are the most likely perturbing entities.

B. Models involving only a single cation vacancy

Figure 3 presents three possibilities for the actual $\text{Sn}^+(1)$ model. The “ $\text{Sn}^+(1)$ ” core is perturbed in a $\{100\}$ plane by a cation vacancy in either one of the three essentially different positions α , β , and γ . In each case the cation vacancy induces the correct orthorhombic symmetry and may, in principle, lead to a small tipping of the z axis away from the $[001]$ axis. The ESR data and the thermal, optical, and production data give no clue as to which model is the correct one. In fact, it is conceivable that two or three possibilities occur simultaneously, yielding for $\theta=0^\circ$ essentially indistinguishable ESR spectra. That this may be so is a real possibility (Sec. III).

Considering the attractive Coulomb interaction between the anion and cation vacancy, the $\text{Sn}^+(1,\alpha)$ model in Fig. 3 seems the most likely possibility. However, it could be that the cation vacancies are locked into positions β or γ by yet another impurity, very likely a Sn^{2+} ion. In fact, divalent-cation-cation-vacancy complexes tend to form dimers, trimers, etc., and more or less distant dimers may be present even after the routine quenching of the samples from 600°C to room temperature. Of course, the possibilities presented in Fig. 3 are not exhaustive: other impurities may induce the orthorhombic symmetry. In fact, position γ could easily be occupied by a Sn^{2+} ion. Finally,

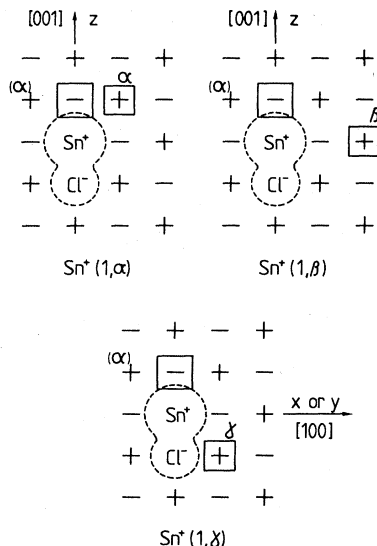


FIG. 3. Three possible single-cation-vacancy models—called $\text{Sn}^+(1,\alpha)$, $\text{Sn}^+(1,\beta)$, and $\text{Sn}^+(1,\gamma)$ —in which the essential “ $\text{Sn}^+(1)$ ” core of Fig. 2 is weakly perturbed in a $\{100\}$ plane by a single cation vacancy inducing the observed orthorhombic symmetry. These centers are only different from one another as long as the vacancies cannot jump. The cation (α) may be replaced by yet another cation vacancy, thus yielding three possible two cation-vacancy models.

considering the fact that Sn^{2+} is easily oxidized to Sn^{4+} , it is possible that oxygen also plays a role.

It should be emphasized that the three models in Fig. 4 are only different as long as the anion and cation vacancies are not able to jump (which they normally can above 220 K). For instance, a single jump by the anion vacancy in the $\text{Sn}^+(1,\gamma)$ model makes it equivalent to $\text{Sn}^+(1,\alpha)$. A single jump of the anion vacancy in $\text{Sn}^+(1,\beta)$ lines up the Sn^+ , the anion, and the cation vacancies, and a tetragonal $\text{Sn}^+(1)$ -type center is formed which has not been observed experimentally.

C. The two-cation-vacancy models

The possibility that the “ $\text{Sn}^+(1)$ ” core of Fig. 3 is perturbed by *two* rather than one cation vacancy must be considered a real one. Indeed, Sn^- centers are produced by x irradiation above 220 K. This process produces two mobile cation vacancies, namely the original charge-compensating one of the Sn^{2+} and the one produced by the site switching of the Sn^0 from the cation position to the anion position before the trapping of the final electron.² Furthermore, a third source of mobile cation vacancies is supplied by the formation of Sn^+ (tetrag) centers.¹ A few possible two-cation-vacancy models can be seen in Fig. 3: the cation indicated by (α) may be replaced by a cation vacancy.

D. The face-diagonal $\text{Sn}^+(1)$ model

One other $\text{Sn}^+(1)$ model needs a short discussion. It is presented in Fig. 4: the “ $\text{Sn}^+(1)$ ” core of Fig. 2 is perturbed in a $\{110\}$ plane by a cation vacancy along the face diagonal in the position δ . Here the cation vacancy would induce orthorhombic symmetry with the x and y axes along perpendicular $\langle 110 \rangle$ directions. No such $\text{Sn}^+(1)$ symmetry is discerned in the ESR spectra and the $\text{Sn}^+(1,\delta)$ model may not exist at all. If so, the reason may be that a single jump, either of the cation vacancy or of the anion vacancy, as indicated in Fig. 4, will yield the $\text{Sn}^+(1,\alpha)$ model of Fig. 3. Such jumps are possible above 220 K for both vacancies unless they are pinned by another impurity.

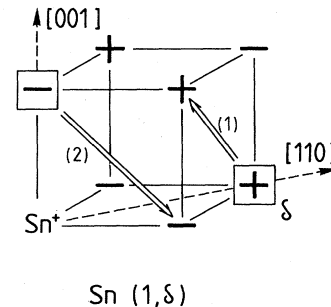


FIG. 4. Schematic three-dimensional representation of another $\text{Sn}^+(1)$ model, called $\text{Sn}^+(1,\delta)$. Such a symmetry—in which the x and y axes are along perpendicular $\langle 110 \rangle$ directions—is not observed. The reason may be that either the cation vacancy makes jump (1), or if it would be locked into its position, the anion vacancy makes jump (2), so that in either case the $\text{Sn}^+(1,\alpha)$ model of Fig. 3 is recovered.

V. PRODUCTION, THERMAL, AND OPTICAL PROPERTIES

An important observation used already in Sec. IV is that $\text{Sn}^+(1)$ is not produced by the x irradiation below 220 K. Above this temperature the anion vacancies (produced simultaneously with halogen interstitials) become increasingly mobile.²⁻⁴ After a Sn^{2+} impurity with a nearby charge-compensation cation vacancy has trapped a mobile electron to form Sn^+ , the latter may stabilize a mobile anion vacancy to form a $\text{Sn}^+(1)$ center.

The production above 220 K is shown in Fig. 5. The crystal was x-irradiated at a given temperature T for 15 min, after which the $\text{Sn}^+(1)$ intensity was measured at 77 K. As an additional experiment the crystal was then irradiated for 5 min at the same temperature T with light from a mercury lamp with an appropriate cutoff filter for exciting F centers (also produced by the x irradiation) at 540 nm. This procedure resulted in a very noticeable increase in the $\text{Sn}^+(1)$ concentration. After this set of measurements the sample was heated to about 600°C for a few minutes in order to destroy all the defects produced by the x irradiation, and the entire procedure was started again at a 10-K-higher temperature.

The two resulting curves are plotted in Fig. 5. It is seen that the $\text{Sn}^+(1)$ center is best formed at 250 K. The observed increase under F bleaching may have two contributing causes. First, the excitation of F centers above 220 K produces both mobile electrons and mobile anion vacancies (which may or may not travel together), and these may be trapped by the Sn^{2+} impurities forming $\text{Sn}^+(1)$ centers. Second, it is possible [similar to the $\text{Tl}^0(1)$ case] that the x irradiation has produced so-called $\text{Sn}^{2+}(1)$ precursor centers, i.e., a Sn^{2+} impurity that has stabilized an anion vacancy. This $\text{Sn}^{2+}(1)$ precursor center may trap a liberated F -center electron producing $\text{Sn}^+(1)$.

The reduced production of $\text{Sn}^+(1)$ above 260 K shown in Fig. 5 is very likely related to its thermal instability. In Fig. 6 the results of a pulse-anneal experiment are presented. The sample was held for 10 min at successive tem-

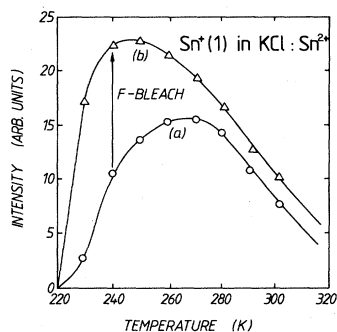


FIG. 5. Production of the $\text{Sn}^+(1)$ center above 220 K. At each indicated temperature the sample was x-irradiated for 15 min, after which the intensity of $\text{Sn}^+(1)$ was recorded at 77 K. Then the sample was F -bleached at the irradiation temperature, and again the observed increase was recorded at 77 K. Then the crystal was heated for a few minutes to 600°C, after which the experiment was restarted at a 10-K-higher temperature.

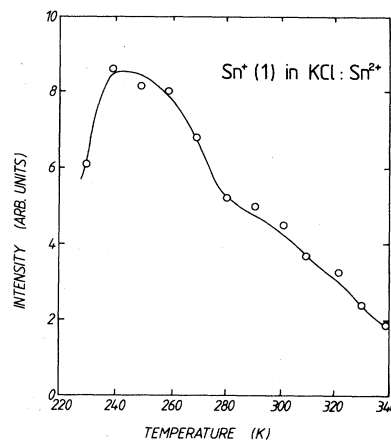


FIG. 6. Pulse-anneal experiment yielding the thermal decay of $\text{Sn}^+(1)$.

peratures (10-K intervals) and each time the changes in $\text{Sn}^+(1)$ intensity were recorded at 77 K. It is seen that $\text{Sn}^+(1)$ decays in the (260–300)-K region corresponding to the decreased production in Fig. 5. The decay mechanism of $\text{Sn}^+(1)$ has not yet been established. It could result either from the simultaneous release of an electron and the anion vacancy (or the divacancy), or from the trapping of a mobile hole or an additional electron.

Finally, the production of $\text{Sn}^+(1)$ as a function of irradiation time at 250 K is presented in Fig. 7. It is seen that $\text{Sn}^+(1)$ reaches its maximum concentration after a 10-min x irradiation, after which it slowly decreases. This slow decrease may be attributed to the fact that $\text{Sn}^+(1)$ is already slightly unstable at 250 K (see Fig. 6).

VI. HYPERFINE INTERACTION OF THE np^1 ($n=4,5,6$) ATOM AND ION CENTERS

Except for $\text{Ge}^+(4p^1)$, which has not yet been observed in KCl, the ESR data, the hf data in particular, on $\text{Sn}^+(1)$ in KCl, more or less complete the long list of np^1 ($n=4,5,6$) heavy-metal atom and ion centers experiencing even and odd crystal fields.^{20,21}

It is worthwhile to review these hf data because they exhibit distinct regularities providing insight into the struc-

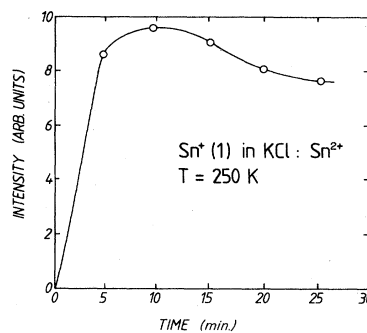


FIG. 7. $\text{Sn}^+(1)$ -center production at 250 K as a function of x-irradiation time.

ture of the defects. Because the spin-orbit interactions are sizable (up to ~ 1 eV for Pb^+), higher-order contributions to the hyperfine components have to be taken into account to second order. The formulas used for diatomic molecules in $^2\Sigma$ ground states²² can be adapted to the problem at hand, i.e., an electron in a p_z orbital. These expressions can be written as a function of the g shifts (2) as follows:

$$A_{\parallel} = A_{\sigma} \left(1 - \frac{1}{2} \Delta g_{\parallel}\right) + \left(2 + \frac{3}{2} \Delta g_{\perp} + \frac{1}{2} \Delta g_{\parallel}\right) \rho, \quad (3)$$

$$A_{\perp} = A_{\sigma} \left(1 - \frac{1}{2} \Delta g_{\parallel}\right) - \left(1 + \frac{13}{4} \Delta g_{\perp} - \frac{9}{4} \Delta g_{\parallel}\right) \rho,$$

in which

$$\rho = \frac{2}{5} \frac{\mu_I}{I} \langle r^{-3} \rangle_{np}$$

is the anisotropic contribution of the np orbital to the hf components, and A_{σ} is the isotropic one. The latter can have two discernible components, namely the exchange polarization contribution A_{σ}^e , which can have either sign, and a positive contribution when ($\mu_I > 0$)

$$A_{\sigma}^s = \frac{8\pi}{3} \frac{\mu_I}{I} |\psi_s(0)|^2$$

caused by s mixing in the ground state.

In order to be able to apply Eqs. (3) to the experimental data, one needs to know the signs of A_{\parallel} and A_{\perp} . By carefully considering all the sign combinations it was established for all the Tl^0 , In^0 , Ga^0 , and Pb^+ centers that

$A_{\parallel} > 0$ and $A_{\perp} < 0$, while, for the Sn^+ centers, $A_{\parallel} < 0$ and $A_{\perp} > 0$. The only reason for this apparently different behavior is that the nuclear moments of the odd Sn nuclei are negative, while they are positive for the Tl, In, Ga, and Pb nuclei. The criterion for the correct sign assignment is whether the experimental ρ value derived from Eqs. (3) compares well with the calculated ρ value using the theoretical $\langle r^{-3} \rangle_{np}$ value obtained from atomic-structure calculations.²³

The results of the analysis are presented in Table II. For the light Ga^0 centers the accuracy of the ρ and A_{σ} values is estimated to be about 2%, while it may increase to 10% for the heavier Tl^0 and Pb^+ centers. In our reanalysis we changed the signs of the A_{\perp} values of $\text{Ga}^0(1)$ and $\text{In}^0(1)$, as given in Table II of Ref. 13, to -5.2 and -7.6 mT, respectively. Despite the discussion in Ref. 13, we believe that these new sign assignments are to be preferred because they lead to better ρ values. Furthermore, there is a misprint in Table IV of Ref. 13: all signs of the hf components of $\text{Ga}^0(\text{axial})$ and $\text{In}^0(\text{ortho})$ should be systematically reversed.

In Table II we have also indicated the "parity" of the crystal field experienced by those centers whose microscopic geometric structure is well established. Two conclusions can be drawn. First, it is seen by inspecting the A_{σ} values that for all the centers possessing inversion symmetry (even crystal field) the unpaired-electron-spin density in the nucleus is large and negative and thus predominantly caused by exchange polarization. It is reasonable to assume that this holds true for the free np^1

TABLE II. Anisotropic part ρ and isotropic part A_{σ} of the hyperfine interaction in various np^1 ($n=4,5,6$) heavy-metal-ion centers in KCl. The values correspond to $^{119}\text{Sn}^+(5p^1)$, $^{207}\text{Pb}^+(6p^1)$, $^{71}\text{Ga}^0(4p^1)$, $^{115}\text{In}^0(5p^1)$, and $^{205}\text{Tl}^0(6p^1)$. When known, the presence or absence of an odd crystal-field component is also given.

Center ^a	ρ (mT)	A_{σ} (mT)	Crystal field	Reference
$\text{Tl}^0(1)$	+96.9	+75.7	odd	5
$\text{Tl}^0(2)$	+101.2	-186	even	5
$\text{In}^0(0) \equiv \text{InCl}_2^{2-}$	+13.3	-10.2	even	13
$\text{In}^0(1)$	+12.6	+10.8	odd	13
$\text{In}^0(2)$	+10.5	-20.3	even	13
$\text{In}^0(\text{ortho})$	+10.3	-18.6		13
$\text{Ga}^0(0) \equiv \text{GaCl}_2^{2-}$	+8.9	-6.3	even	13
$\text{Ga}^0(1)$	+8.9	+5.0	odd	13
$\text{Ga}^0(2)$	+7.5	-13.1	even	13
$\text{Ga}^0(\text{axial})$	+7.9	-13.3		13
$\text{Sn}^0(0) \equiv \text{SnCl}_2^-$	-39.3 ^b	+19.5 ^b	even	1
$\text{Sn}^+(1)$	-32.7 ^b	+2.9 ^b	odd	this paper
Pb^+	+76.0	-96.4	even(?)	20

^aThe number 0, 1, or 2 in parentheses indicates the number of anion vacancies present in the center (Ref. 5).

^bThe nuclear moments of the odd tin isotopes are negative, whereas they are positive for the other heavy-metal nuclei. As a result, the positive A_{σ} values for ^{117}Sn also correspond to a negative unpaired-electron-spin density at the nucleus.

($n=4,5,6$) atoms and ions, although clearly the size may be somewhat different. Second, the A_σ values of the centers which experience an odd crystal-field component, i.e., $\text{Tl}^0(1)$, $\text{In}^0(1)$, $\text{Ga}^0(1)$, and $\text{Sn}^+(1)$, are substantially larger than for the previous centers. This is undoubtedly caused by the s mixing induced by the odd crystal-field component, and as a result a sizeable positive contribution A_σ^s is added to the negative A_σ^e value characteristic of the free atom or ion. This effect is so pronounced that it may be used as an argument in deciding between several possible center models that may be associated with a given np^1 heavy-metal ESR spectrum. A case in point is provided by the $\text{Pb}^+(6p^1)$ ESR spectra in KCl that are currently being investigated in our laboratory.

VII. CONCLUDING REMARKS

In this paper we have established that in $\text{KCl}:\text{Sn}^{2+}$ crystals $\text{Sn}^+(1)$ centers can be produced whose essential structural core corresponds to the laser-active-type structure (Fig. 2), i.e., a substitutional $\text{Sn}^+(5p^1)$ center strongly perturbed by an anion vacancy. The position of the weak-

ly perturbing cation vacancy that must be present cannot be established with certainty, but in our opinion the $\text{Sn}^+(1, \alpha)$ model of Fig. 3 is likely to be a dominantly occurring configuration. The luminescence properties and possible laser activity of $\text{Sn}^+(1)$ centers remain to be studied, and such experiments are presently being prepared. Finally, interesting regularities have been observed in the properties of the hyperfine interaction of the np^1 ($n=4,5,6$) atoms and ions and in the effect of a strong odd axial crystal-field component.

ACKNOWLEDGMENTS

The authors would like to thank A. Bouwen for his skillful experimental assistance. One of us (I.H.) is grateful to the IWONL (Instituut voor Wetenschappelijk Onderzoek in Nijverheid en Landbouw) for financial aid. This work was supported by the IIKW (Interuniversitair Instituut voor Kernwetenschappen), the Geconcerteerde Acties, and the PREST Program (Ministerie van Wetenschapsbeleid), to which the authors are greatly indebted.

¹C. J. Delbecq, R. Hartford, D. Schoemaker, and P. H. Yuster, *Phys. Rev. B* **13**, 3631 (1976).

²F. Van Steen and D. Schoemaker, *Phys. Rev. B* **19**, 55 (1979).

³E. Goovaerts, S. V. Nistor, and D. Schoemaker, *Phys. Rev. B* **25**, 83 (1982).

⁴F. Lüty, in *Physics of Color Centers*, edited by W. B. Fowler (Academic, New York, 1968).

⁵E. Goovaerts, J. Andriessen, S. V. Nistor, and D. Schoemaker, *Phys. Rev. B* **24**, 29 (1981); D. Schoemaker, E. Goovaerts, and S. V. Nistor, *Bull. Am. Phys. Soc.* **23**, 200 (1978).

⁶S. V. Nistor, E. Goovaerts, A. Bouwen, and D. Schoemaker, *Phys. Rev. B* **27**, 5797 (1983).

⁷P. G. Baranov and V. A. Khramtsov, *Phys. Status Solidi B* **101**, 153 (1980).

⁸L. F. Mollenauer, N. D. Vieira, and L. Szeto, *Phys. Rev. B* **27**, 5332 (1983).

⁹F. J. Ahlers, F. Lohse, J. M. Spaeth, and L. F. Mollenauer, *Phys. Rev. B* **28**, 1249 (1983).

¹⁰W. Gellerman, F. Lüty, and R. C. Pollock, *Opt. Commun.* **39**, 391 (1981).

¹¹L. F. Mollenauer, N. D. Vieira, and L. Szeto, *Opt. Lett.* **7**, 414 (1982).

¹²L. F. Mollenauer and R. H. Stolen, *Opt. Lett.* **9**, 13 (1984).

¹³W. Van Puymbroeck, J. Andriessen, and D. Schoemaker, *Phys. Rev. B* **24**, 2412 (1981).

¹⁴W. Van Puymbroeck, D. Schoemaker, and J. Andriessen, *Phys. Rev. B* **26**, 1139 (1982).

¹⁵N. D. Vieira, L. F. Mollenauer, and L. H. Szeto, *Solid State Commun.* **50**, 1037 (1984).

¹⁶F. J. Ahlers, F. Lohse, Th. Hangleiter, J. M. Spaeth, and R. H. Bartram, *J. Phys. C* **17**, 4877 (1984).

¹⁷D. Schoemaker and J. L. Kolopus, *Solid State Commun.* **8**, 435 (1970).

¹⁸N. I. Melnikov, R. A. Zhitnikov, and V. A. Khramtsov, *Fiz. Tverd. Tela (Leningrad)* **17**, 3234 (1975) [*Sov. Phys.—Solid State* **17**, 2129 (1976)].

¹⁹W. Van Puymbroeck and D. Schoemaker, *Phys. Rev. B* **23**, 1670 (1981); W. Van Puymbroeck, N. Schrijvers, A. Bouwen, and D. Schoemaker, *Phys. Status Solidi B* **112**, 725 (1982).

²⁰E. Goovaerts, S. V. Nistor, and D. Schoemaker, *Phys. Rev. B* **28**, 3712 (1983).

²¹B. R. Yang, E. Goovaerts, and D. Schoemaker, *Phys. Rev. B* **27**, 1507 (1983).

²²D. Schoemaker, *Phys. Rev. B* **7**, 786 (1973).

²³S. Fraga, J. Karkowski, and K. M. S. Saxena, *Handbook of Atomic Data* (Elsevier, Amsterdam, 1976).